# Updating the mass calibration of the Planck cluster sample


*Gaspard Aymerich*

*Marian Douspis, Laura Salvati*
Institut d'Astrophysique Spatiale, Université Paris-Saclay

*Gabriel Pratt*
Astrophysique Interactions Multi-Echelles, CEA



A&A, 690, A238
arXiv:2509.08673
arXiv:2509.02068


*CMB-France #7*
*14/10/2025*

# Formation of galaxy clusters

Gravitational collapse & expansion of Universe:
Formation of a cosmic web, with extreme overdensities at the nodes, **galaxy clusters**

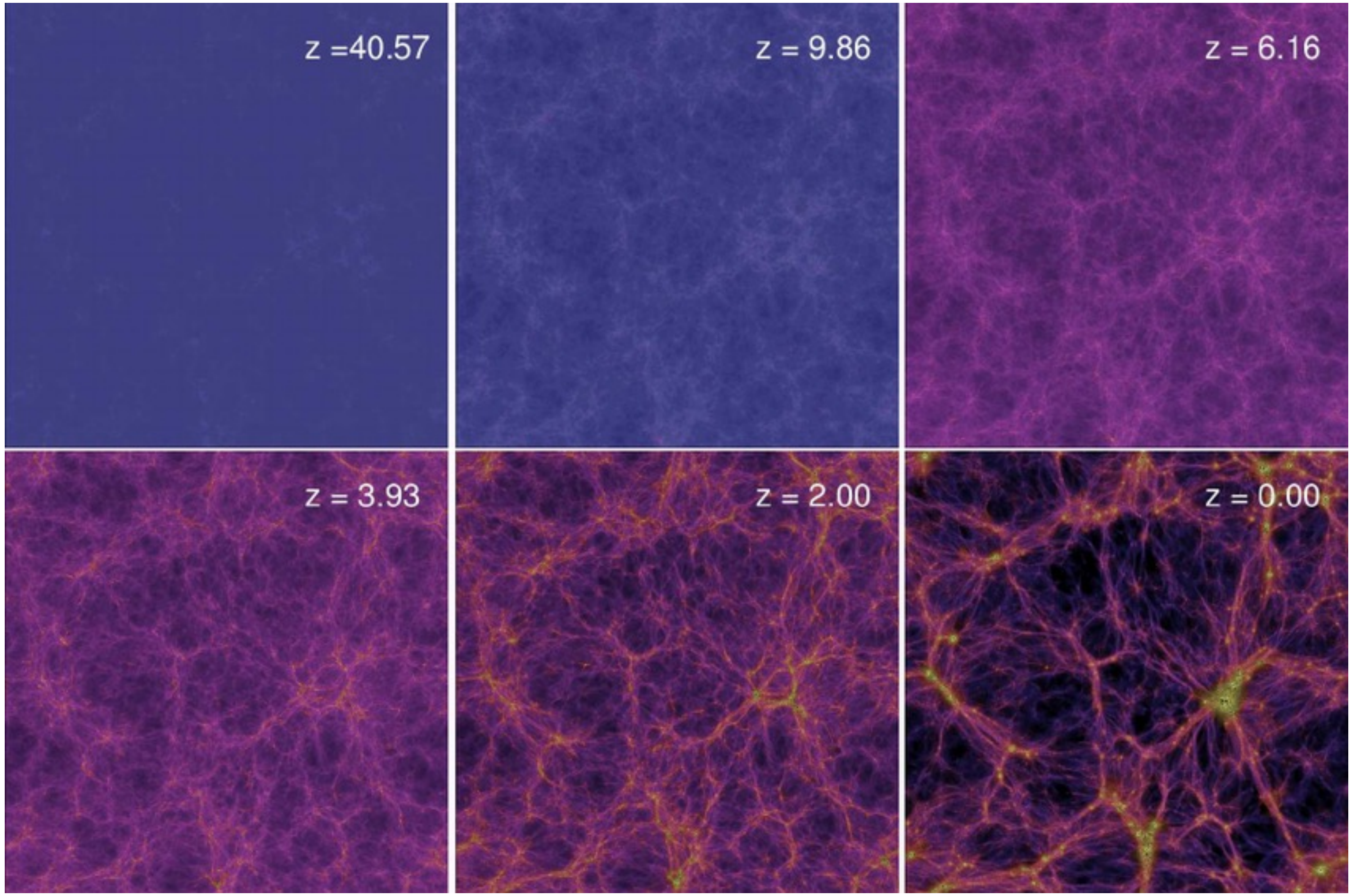

Zhao et al. 2012

« Typical » galaxy cluster:
1 Mpc, $5.10^{14} M_{\odot}$

80% dark matter
16% hot gas (>1 keV)
4% stars

# Galaxy clusters & cosmology

How can galaxy clusters be used as a cosmological probe ?

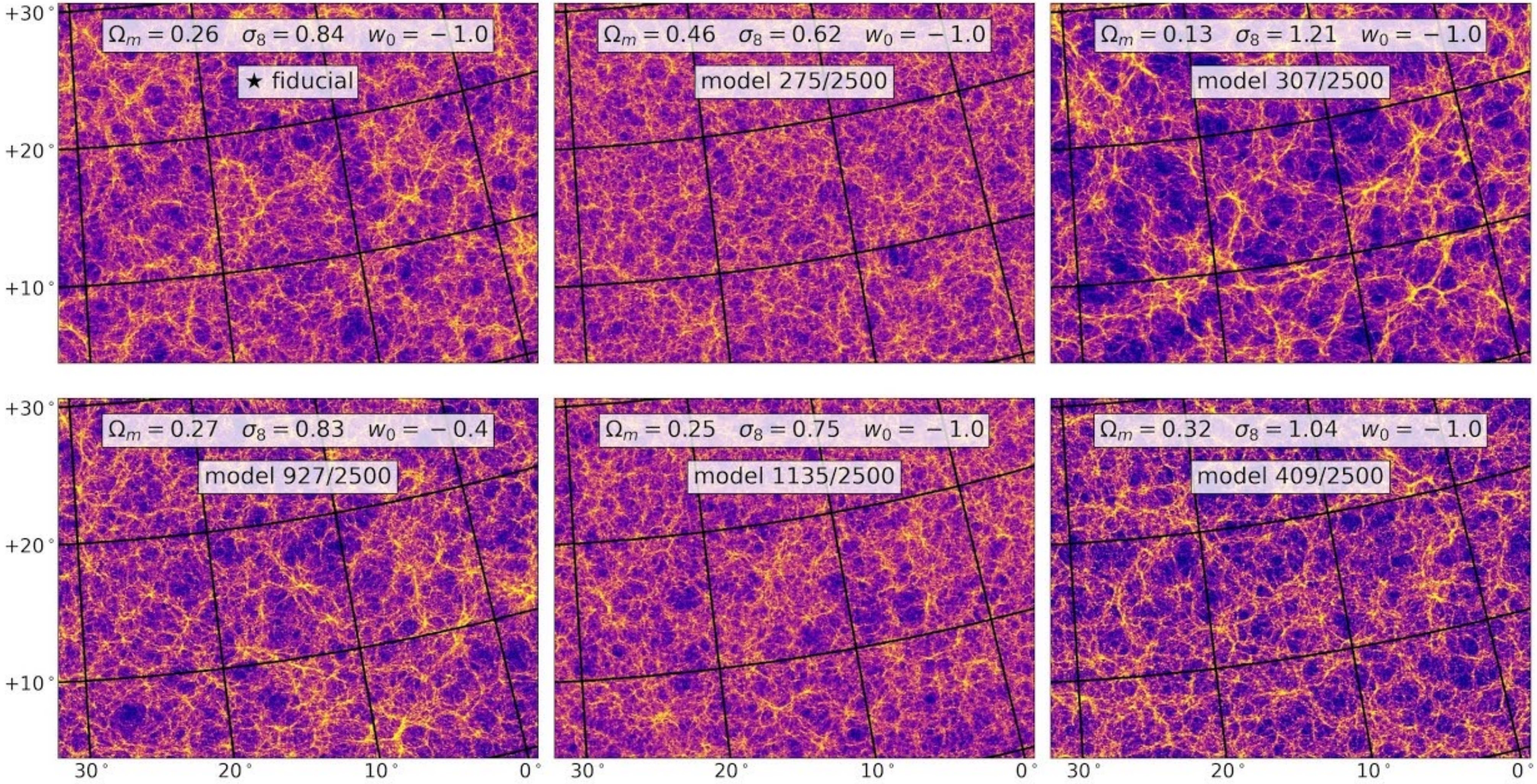


cosmogrid.ai

The formation of structures depends on the underlying cosmological model,
leading to **different populations of galaxy clusters**

# Galaxy clusters & cosmology

How can galaxy clusters be used as a cosmological probe ?

Mass function: theoretical **prediction of cluster abundance** as function of **mass and redshift**

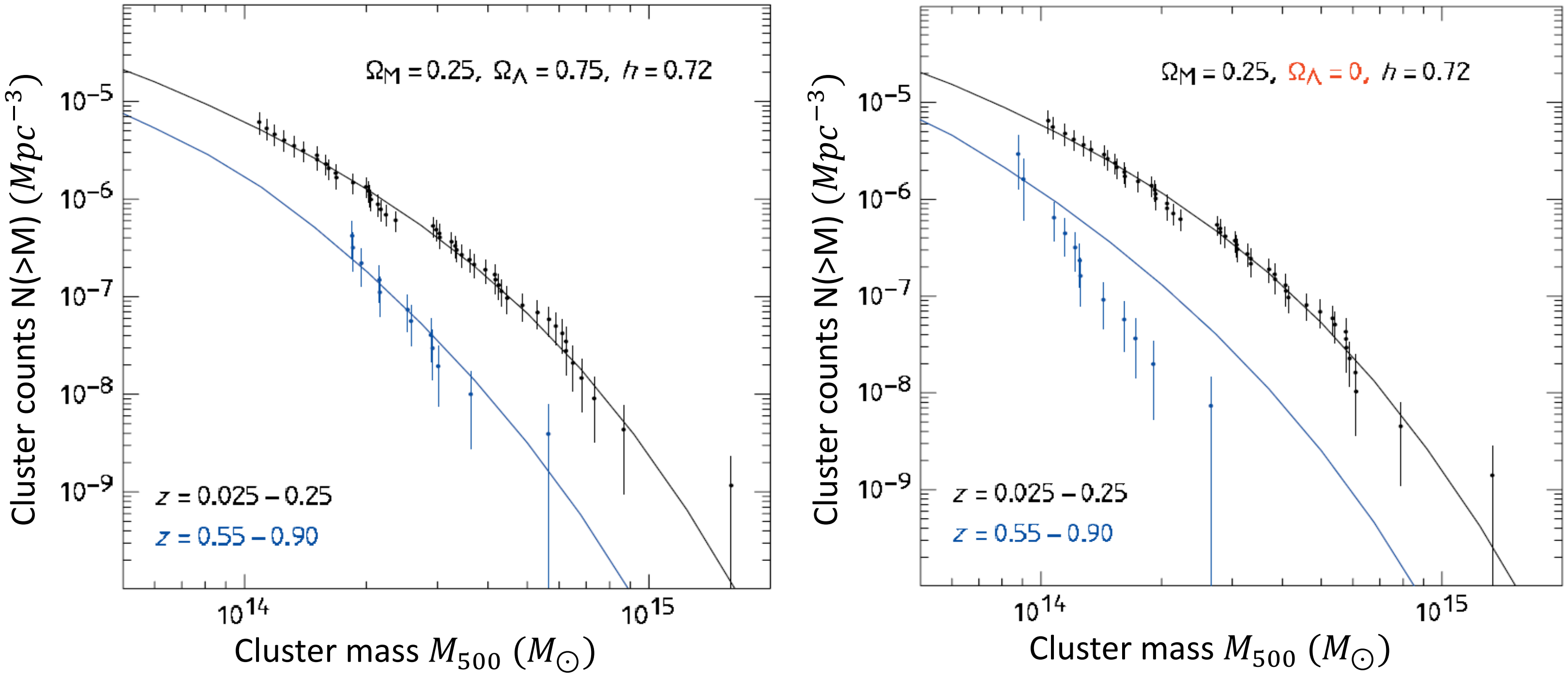


Vikhlinin et al. 2009

3 ingredients in a cluster analysis:

| Systematically detected sample (with known selection function) | Link between halo mass and observables | Cosmology-dependent mass function |
|---|---|---|

## How can galaxy clusters be used as a cosmological probe ?

Mass function: theoretical **prediction of cluster abundance** as function of **mass and redshift**

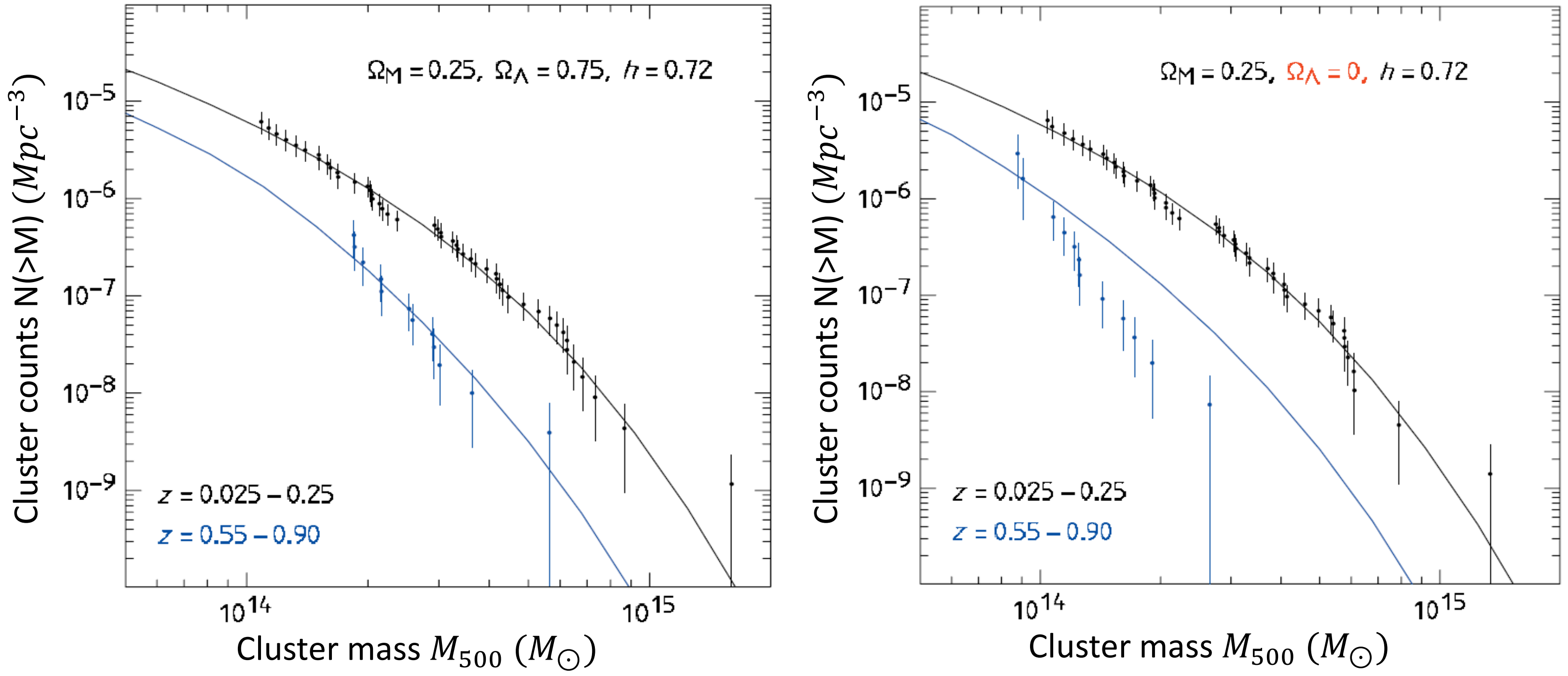


Vikhlinin et al. 2009

3 ingredients in a cluster analysis:

- Systematically detected sample (with known selection function)
- Link between halo mass and observables
- Cosmology-dependent mass function

# Observing galaxy clusters

## How can we observe them ?

**Different wavelengths probe different properties of clusters**

Combining all wavelengths allows for more precise characterisation of cluster properties

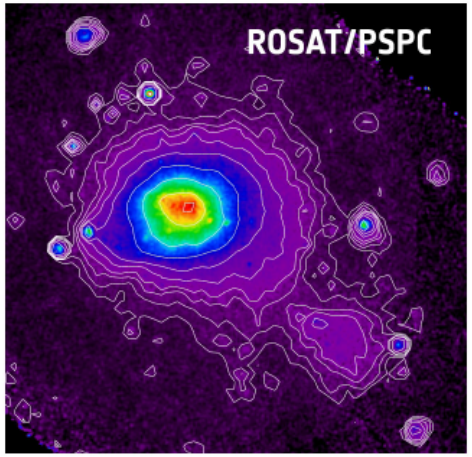


**X-ray** emission:
**Bremmstrahlung**
Sensitive to **gas density squared**
High resolution

$$E_X \propto \int_V n_e^2 \Lambda(T) dV$$

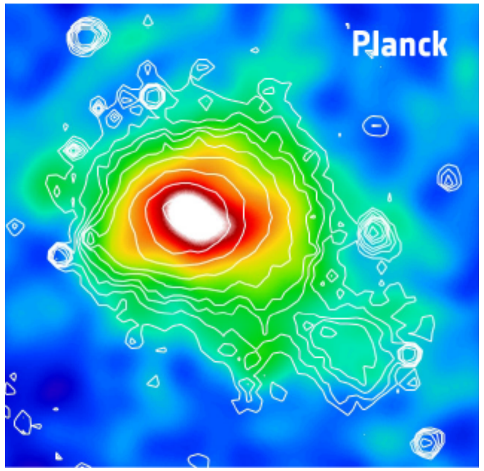


**mm**-wavelength:
**Thermal Sunyaev-Zeldovich effect**
(inverse Compton scattering)
Sensitive to **gas pressure**

$$F_\nu \propto \int_\Omega (P = n_e T) d\Omega$$


**Optical/near IR** wavelength:
**Stars** (small part of total mass)
**Gravitational lensing**
(total mass, limited precision)

# The Planck cluster sample

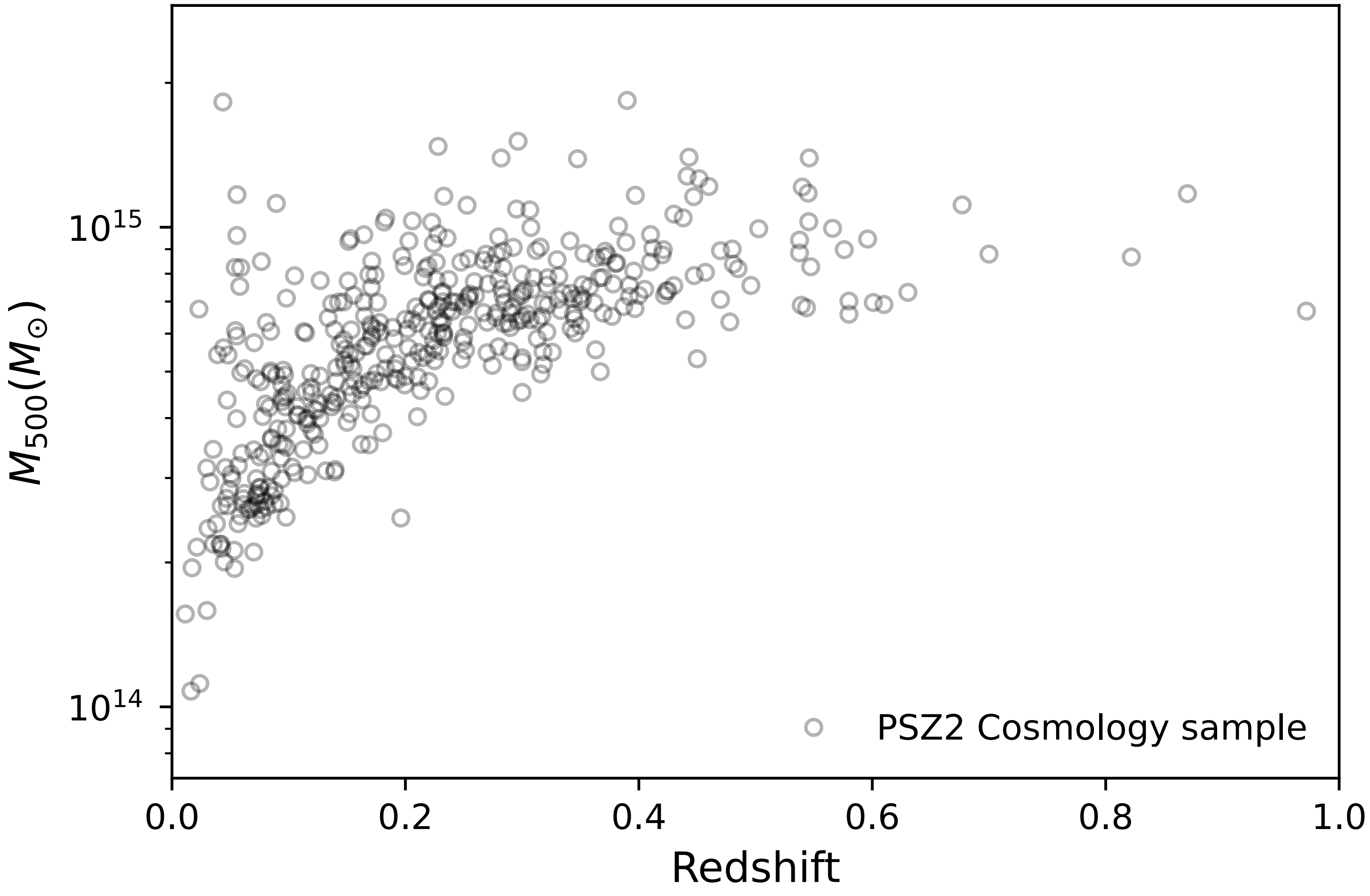


439 SZ-detected clusters with spectroscopic redshifts
in the cosmological sample

# Original Planck approach

## Two-step observable-mass relation

Arnaud et al. 2010 relates X-ray signal from XMM-Newton to mass under hydrostatic equilibrium assumption

Y500-M500 is calibrated on a common XMM/SZ set of 71 clusters: $E^{-2/3}(z)\left[\frac{D_A^2\, Y_{500}}{10^{-4}\,\mathrm{Mpc}^2}\right] = 10^{-0.19\pm0.02}\left(\frac{(1-b)\,M_{500}}{6\times10^{14}\,M_\odot}\right)^{1.79\pm0.08}$

$(1-b)$, the hydrostatic mass bias, is calibrated with WL data, which was very limited at the time (2 samples with around 25 clusters + experimental CMB lensing)

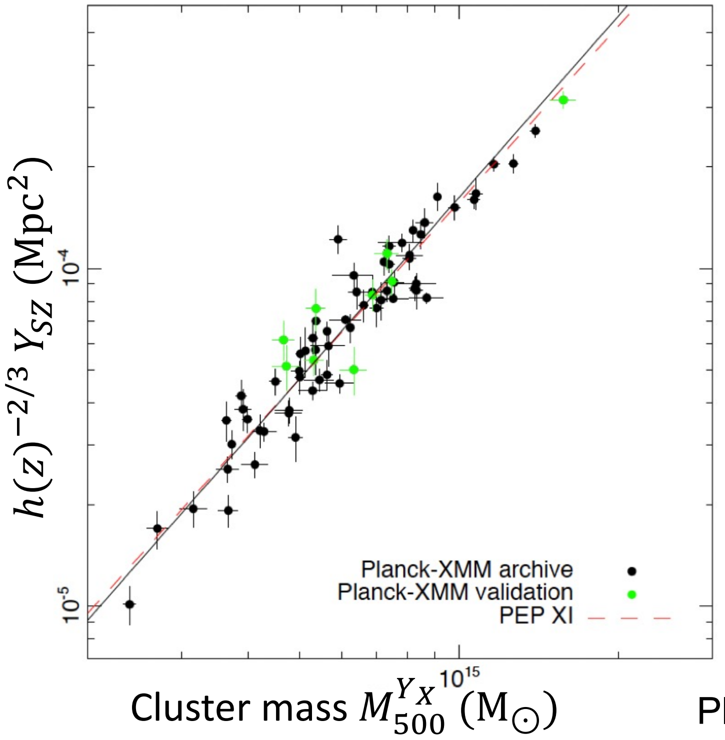


Planck 2013

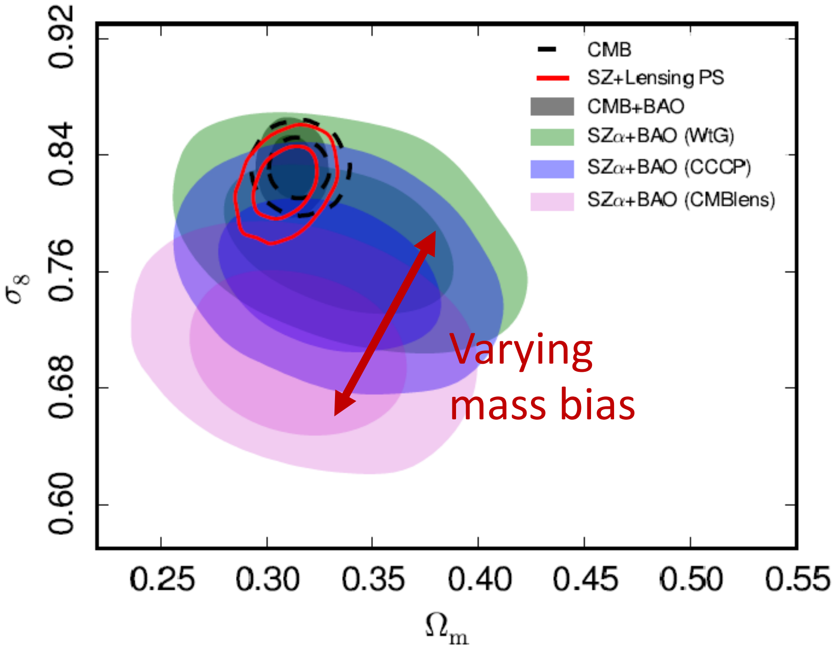


Planck 2015

# Updating the calibration samples

## X-ray calibration sample

~~Arnaud et al. 2010 relates X-ray signal from XMM-Newton~~ to mass under hydrostatic equilibrium assumption

~~Y500-M500 is calibrated on a common XMM/SZ set of 71 clusters:~~ $E^{-2/3}(z)\left[\frac{D_A^2\, Y_{500}}{10^{-4}\,\mathrm{Mpc}^2}\right] = 10^{-0.19\pm0.02}\left(\frac{(1-b)\,M_{500}}{6\times10^{14}\,M_\odot}\right)^{1.79\pm0.08}$

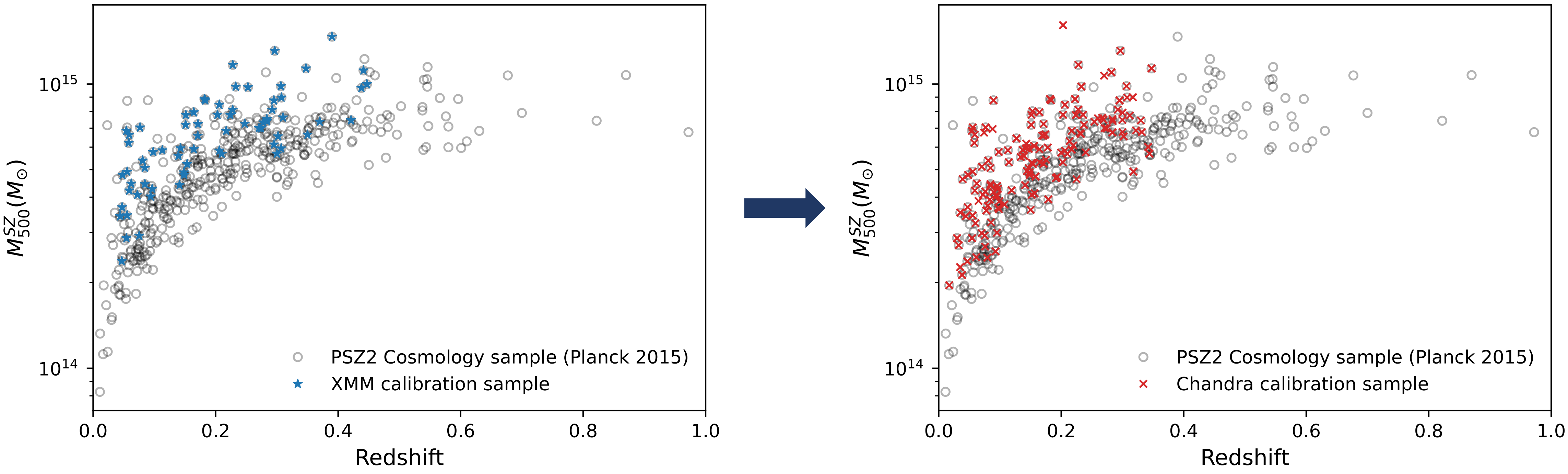

# Updating the calibration samples

## X-ray calibration sample

Vikhlinin et al. 2009 relates X-ray signal from Chandra to mass under hydrostatic equilibrium assumption

~~Y500-M500 is calibrated on a common XMM/SZ set of 71 clusters:~~ $E^{-2/3}(z)\left[\frac{D_A^2\, Y_{500}}{10^{-4}\,\mathrm{Mpc}^2}\right] = 10^{-0.19\pm0.02}\left(\frac{(1-b)\,M_{500}}{6\times10^{14}\,M_\odot}\right)^{1.79\pm0.08}$

**Full re-observation of Planck ESZ sample (with z<0.35) by Chandra**

SZ-selected sample
More clusters (146 vs 71)
Better low-mass leverage
Similar high-mass leverage
Better low-redshift leverage
Slightly worse high-redshift leverage

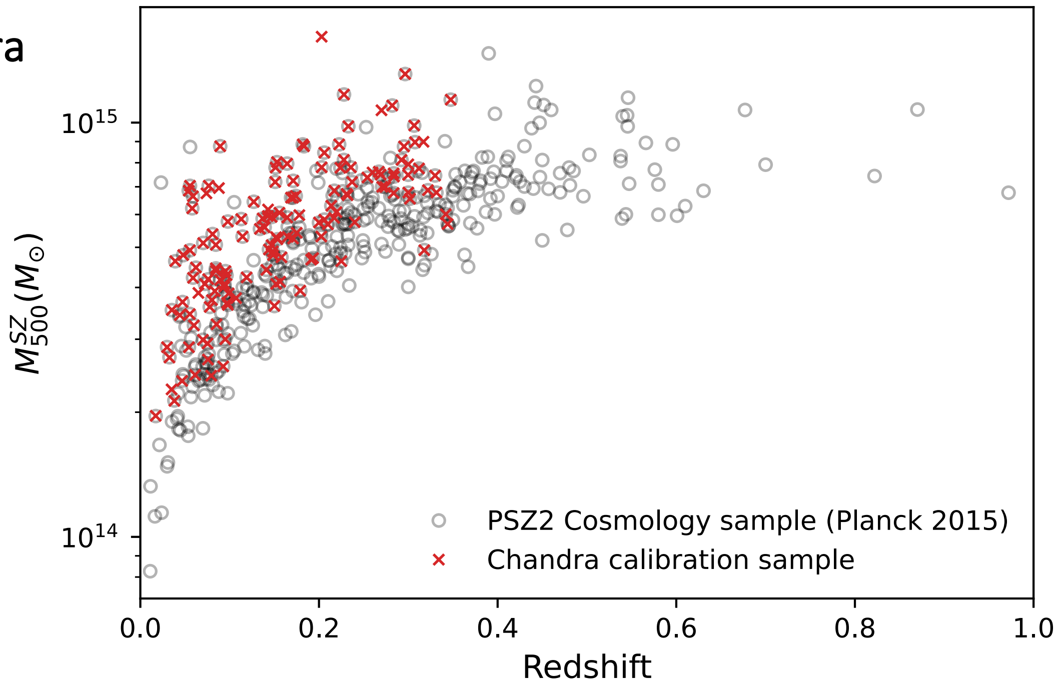

# Updating the calibration samples

## Calibrating the Ysz-M relation

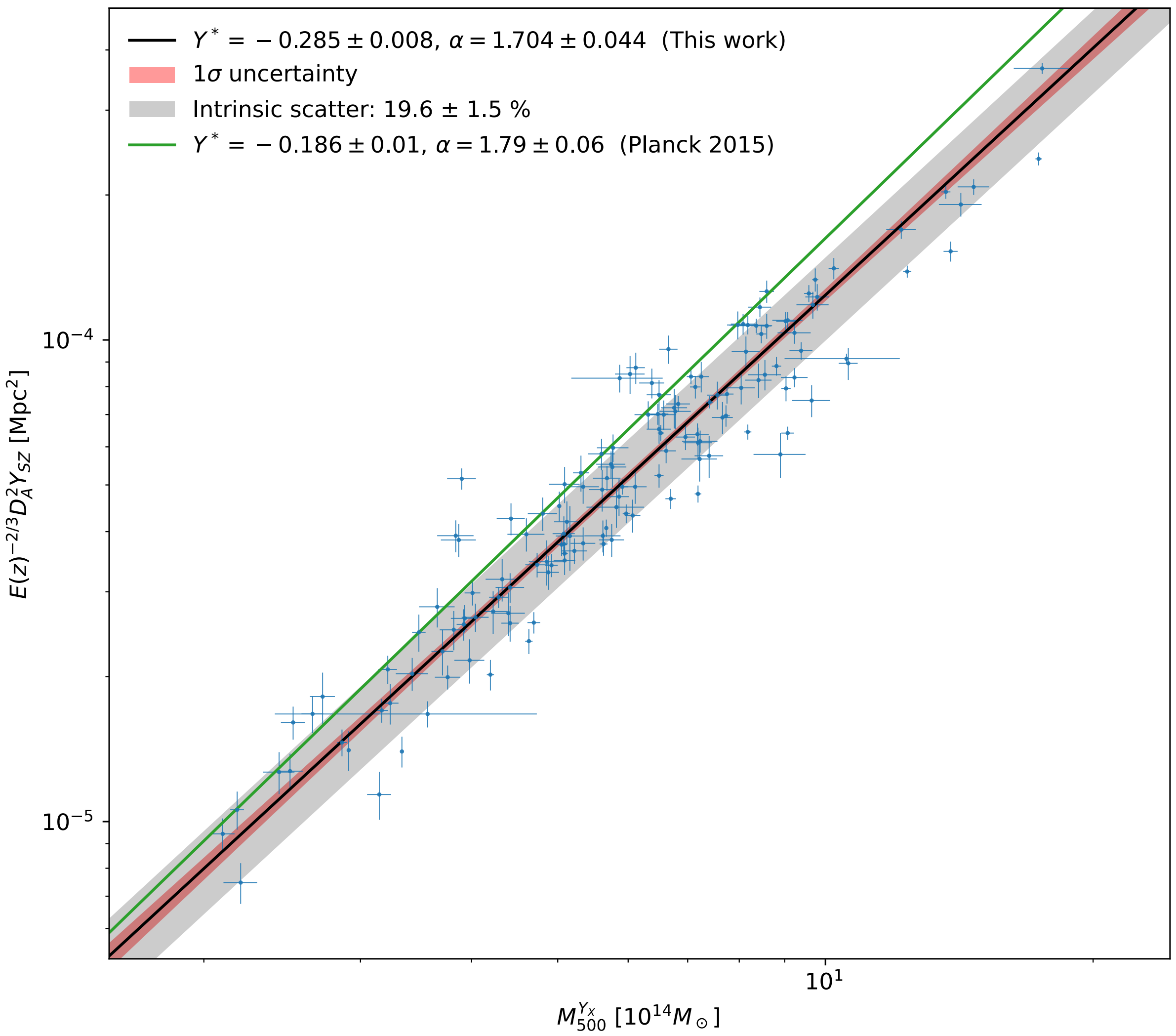


Run **MMF algorithm with X-ray positions and apertures**
Obtain Ysz with uncertainties

**Correct for Malmquist bias**:
Divide each individual Ysz by mean bias at that value

After **adding statistical uncertainty and scatter from X-ray scaling relation**:

$$E^{-2/3}(z)\frac{D_A^2\, Y_{500}}{10^{-4}\mathrm{Mpc}^2} = 10^{-0.29\pm0.01}\left(\frac{(1-b)M_{500}}{6\cdot10^{14}M_\odot}\right)^{1.70\pm0.1}$$

Scatter: 21%

**Robust to fitting method** (emcee, LinMix, BCES)

# Updating the calibration samples

## Comparison with Planck 2015

Chandra scaling relation:

$$E^{-2/3}(z)\frac{D_A^2\,Y_{500}}{10^{-4}\mathrm{Mpc}^2} = 10^{-0.29\pm0.01}\left(\frac{(1-b)M_{500}}{6\cdot10^{14}M_\odot}\right)^{1.70\pm0.1}$$

Scatter: 21%

Planck collab. 2015 Cosmology from SZ number counts scaling relation :

$$E^{-2/3}(z)\left[\frac{D_{\mathrm{A}}^2\,Y_{500}}{10^{-4}\,\mathrm{Mpc}^2}\right] = 10^{-0.19\pm0.02}\left(\frac{(1-b)\,M_{500}}{6\times10^{14}\,M_\odot}\right)^{1.79\pm0.08}$$

Scatter: 18%

The new scaling relation has:
Lower normalization: Chandra and XMM temperature calibration don’t match, Chandra measures hotter and thus heavier cluster. The **difference is coherent with predictions from Schellenberger et al. 2015** (20% difference)

Shallower slope: The new scaling relation is closer to self-similar (slope of 5/3)

**Comparable uncertainties:** Lower uncertainties on $Y_{SZ}$-$M_{Y_X}$ (larger sample) but higher uncertainties on $Y_X$-$M_{Y_X}$ compensates the difference

# Updating the calibration samples

## Calibrating the hydrostatic mass bias

**X-Ray masses are obtained under the assumption of hydrostatic equilibrium** (i.e. thermal pressure perfectly balancing gravity)

Non thermal pressure support and deviations from equilibrium lead to **under-estimation of the true mass**

Effect accounted for by a **multiplicative factor, calibrated with weak lensing mass estimates**

$$E^{-2/3}(z)\,\frac{D_A^2\,Y_{500}}{10^{-4}\mathrm{Mpc}^2} = 10^{-0.29\pm0.01}\left(\frac{(1-b)M_{500}}{6\cdot 10^{14}M_\odot}\right)^{1.70\pm0.1}$$

Two data sets:

- Pointed WL data from Herbonnet et al. 2020
- Wide-field WL data from DES

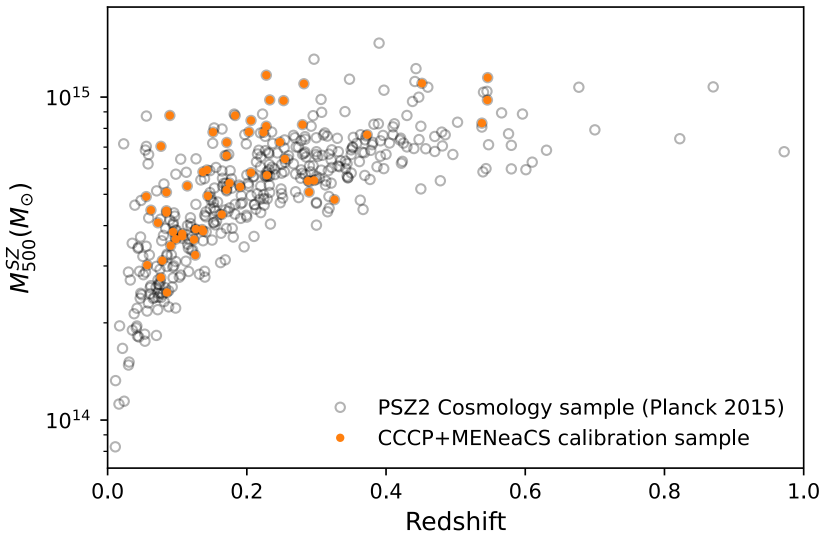


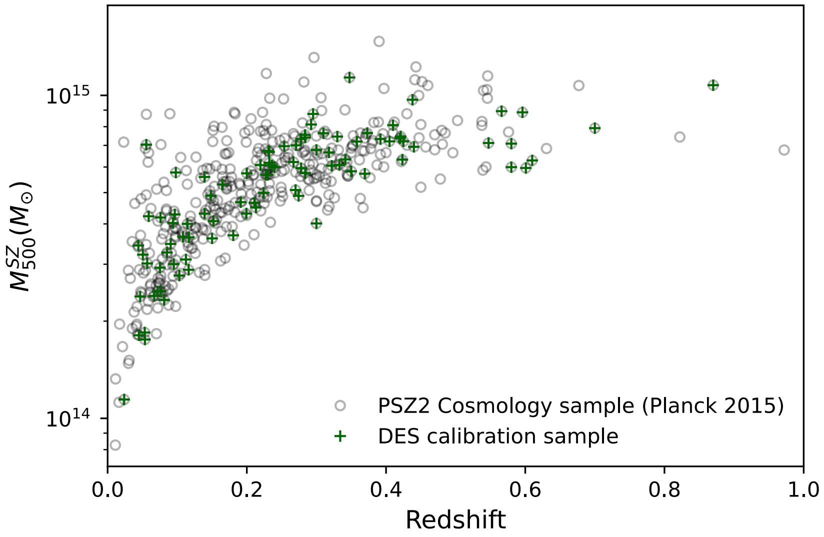

## Calibrating the hydrostatic mass bias

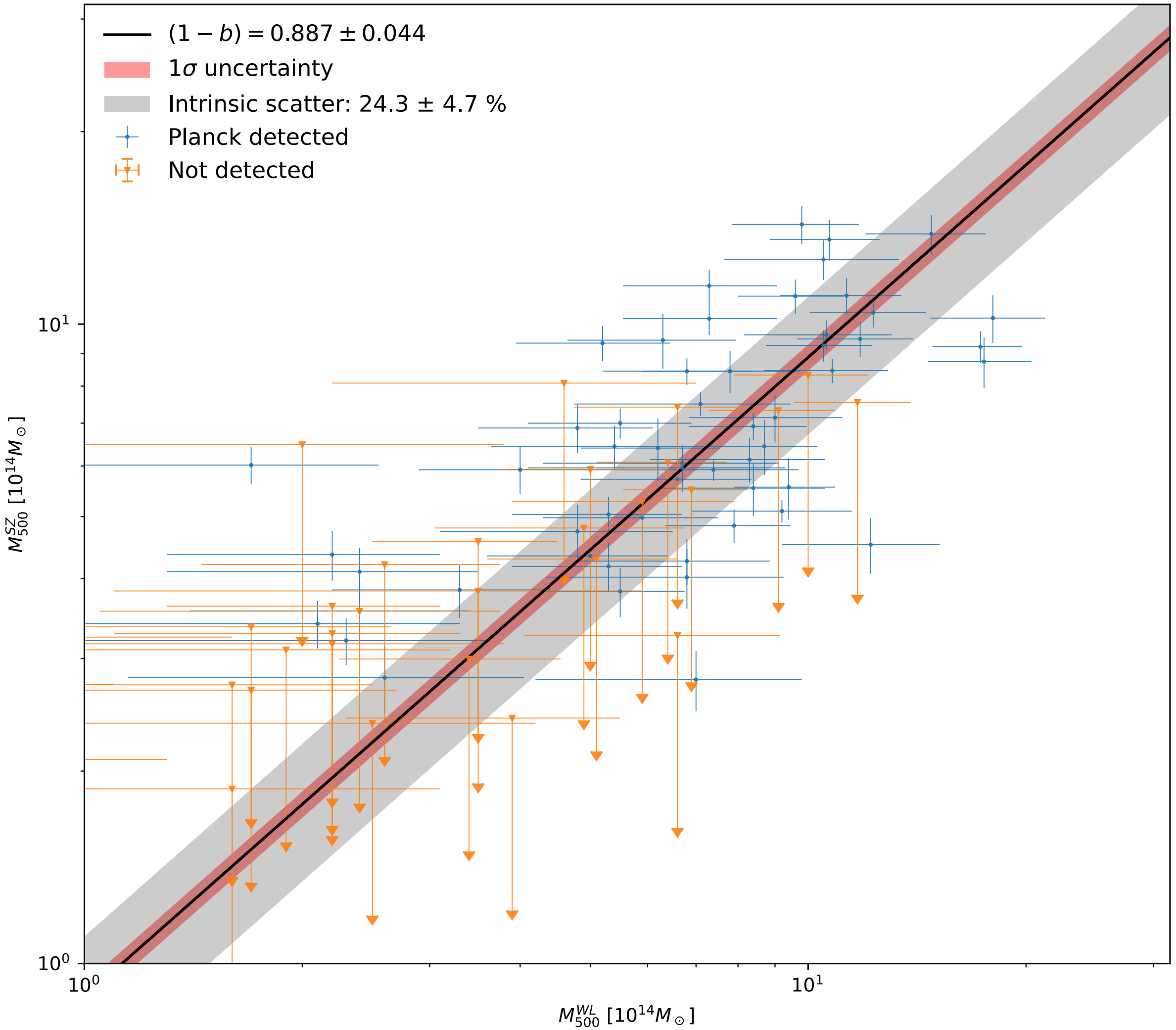


**56 matches** between Herbonnet et al. and PSZ2 catalogues

**36 clusters** with WL data undetected by Planck, take them into account in the bias calibration

| Calibration sample | D+nD | D |
|---|---|---|
| Chandra | $0.89 \pm 0.04$ | $0.91 \pm 0.05$ |
| XMM-Newton | $0.76 \pm 0.04$ | $0.78 \pm 0.04$ |
| Herbonnet+20 | X | $0.81 \pm 0.04$ |
| CCCP (P15) | X | $0.78 \pm 0.09$ |

# Internal mass calibration with DES

## Weak-lensing likelihood

Hydrostatic masses are biased, need to correct them with WL data

Tangential shear profile → $\hat{g}^i_t$

Hydro mass from Ysz + Xray scaling relation → $M^i_H$

$$\mathcal{L}^i = P(\hat{g}^i_t | M^i_H, z^i) = \frac{P(\hat{g}^i_t, M^i_H | z^i)}{P(M^i_H | z^i)}$$

Assuming scatter-less mass bias, i.e. $P(M^i_H | M, z^i) = \delta(M^i_H - (1-b)M)$

The likelihood can be written as:

$$\mathcal{L}^i = \int \mathrm{d}M_{WL} P(\hat{g}^i_t | M_{WL}, z^i) P(M_{WL} | M = \frac{M^i_H}{1-b}, z^i)$$

Lensing model based on NFW model → $P(\hat{g}^i_t | M_{WL}, z^i)$

Takes WL mass bias into account → $P(M_{WL} | M = \frac{M^i_H}{1-b}, z^i)$

The WL likelihood is simultaneously sampled with the cosmology

# Cosmological constraints

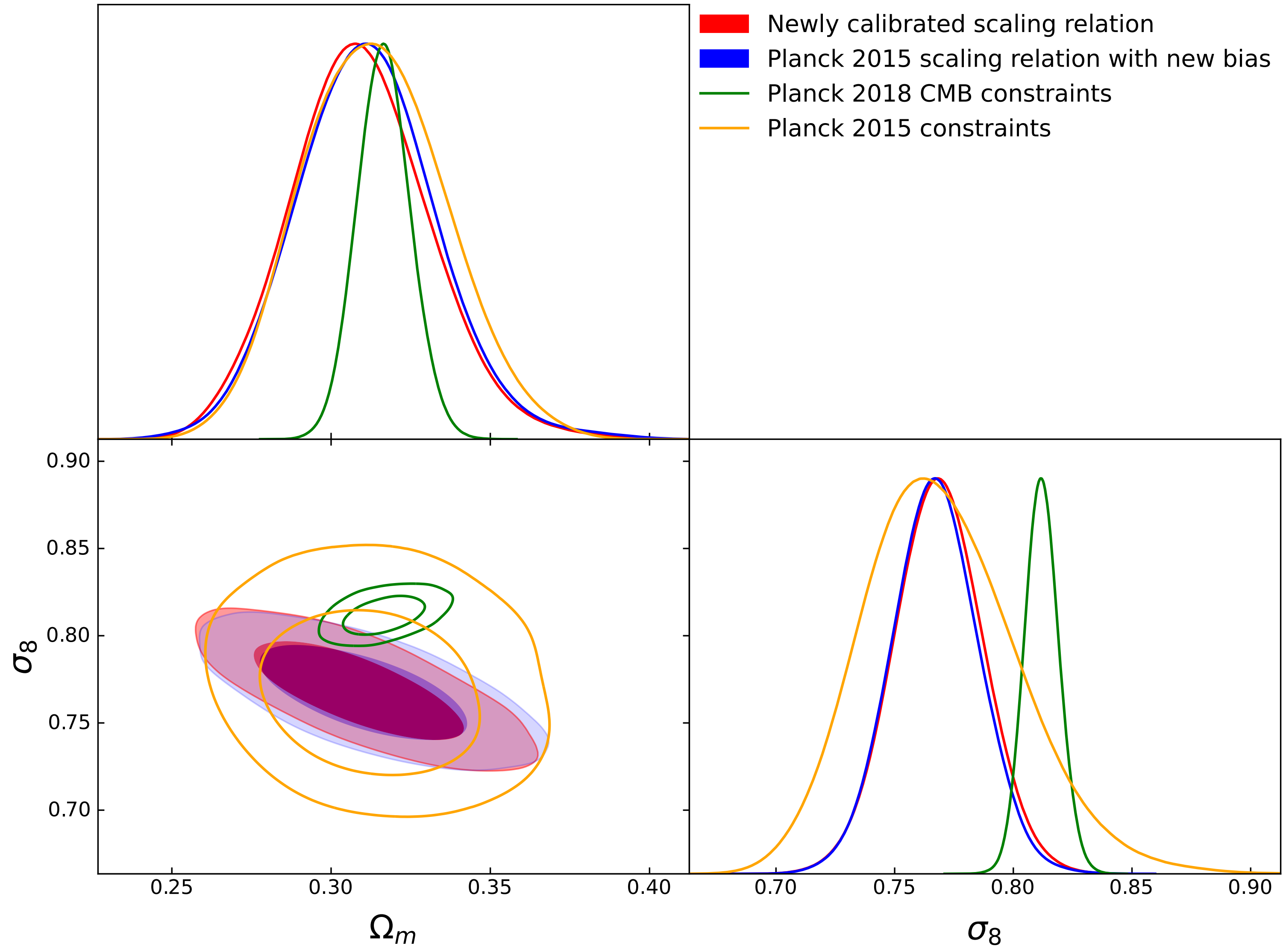


The X-ray calibration sample doesn't change the final results
Constraints are coherent but tighter than previous Planck results

# Cosmological constraints

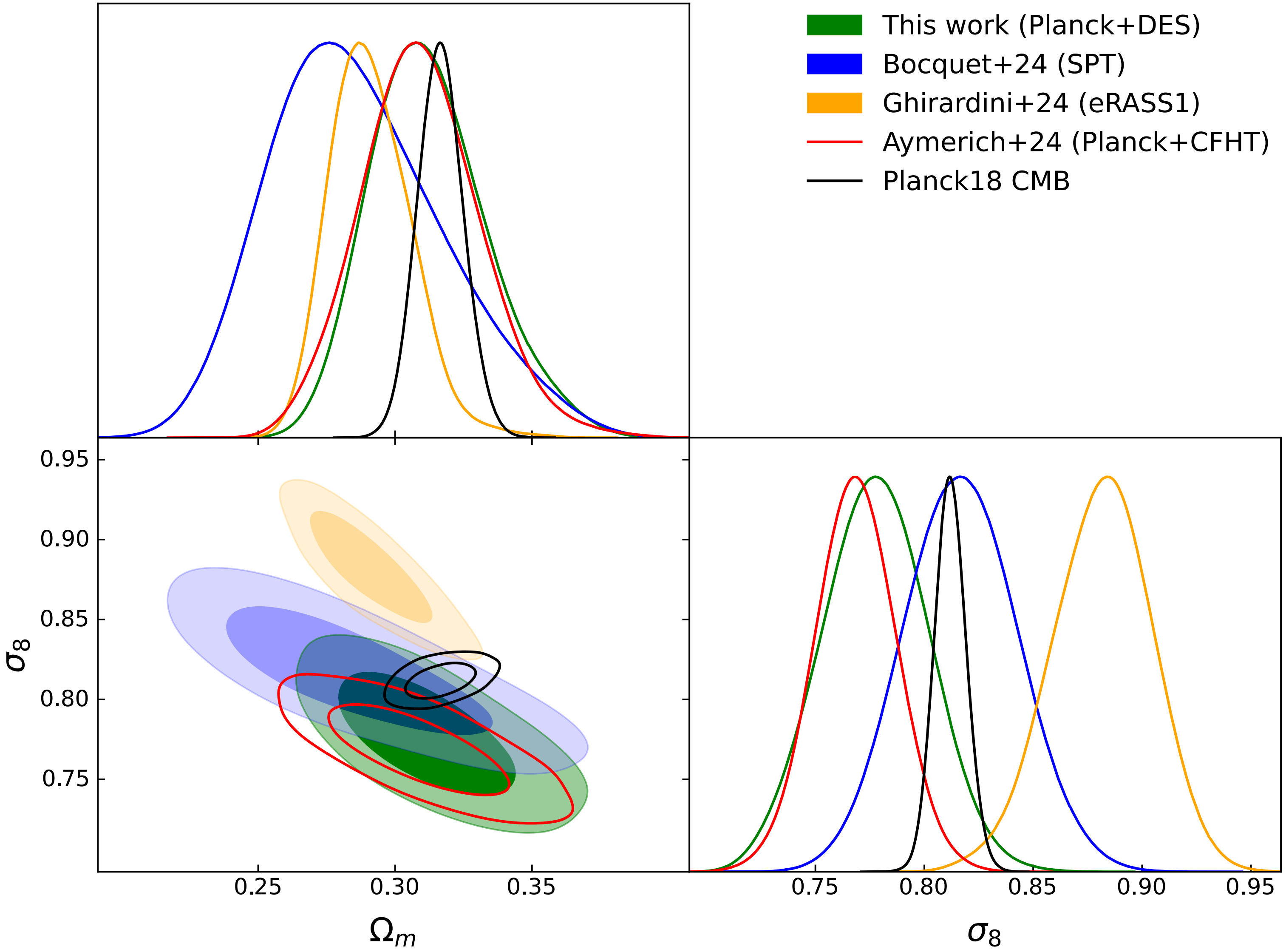


Our results are in reasonable agreement with SPT and Planck CMB, and in 2.9$\sigma$ tension with eRASS1 results

# Cosmological constraints

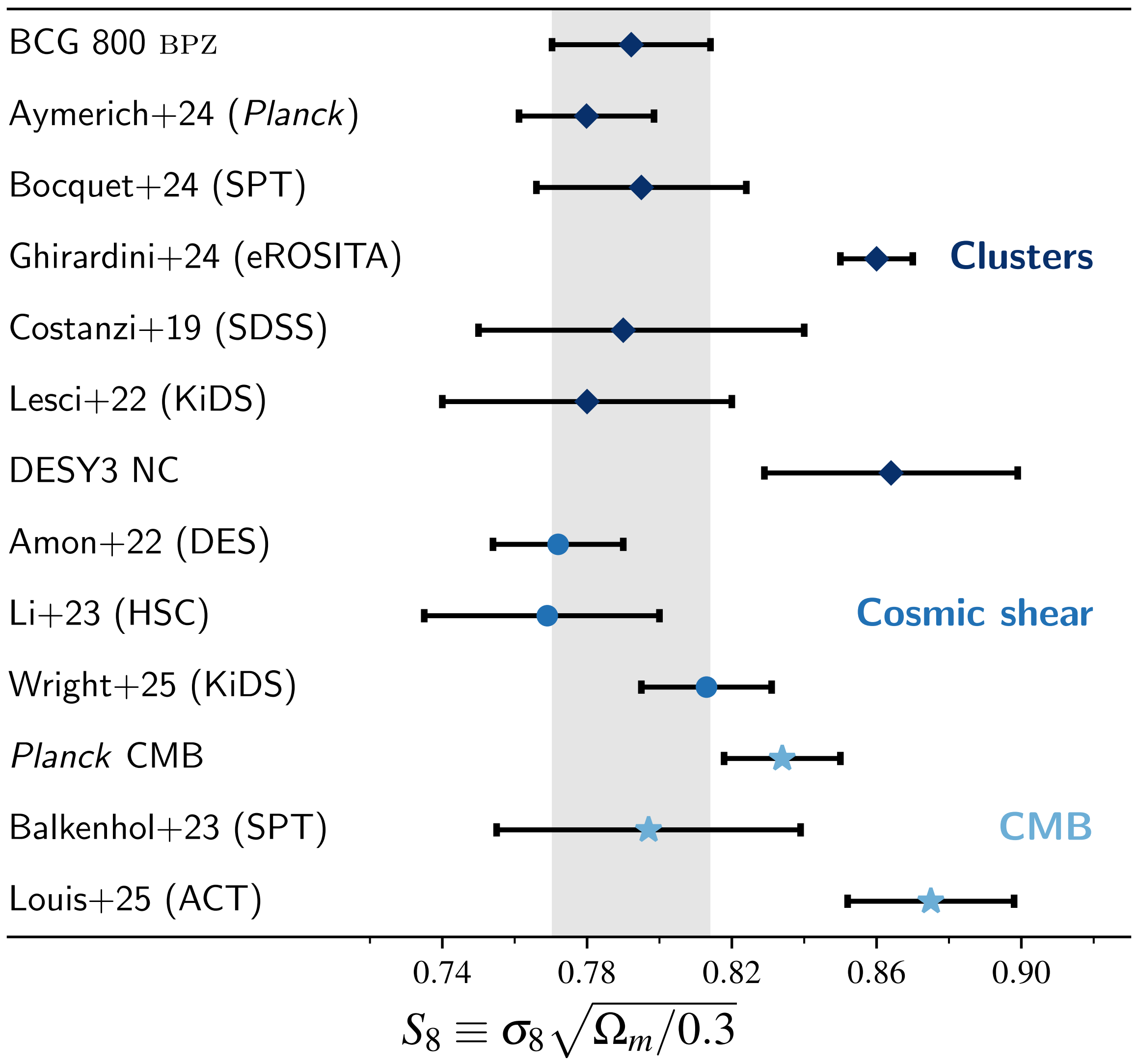


With the same mass calibration, tension between Planck SZ and eRASS1 constraints remains
Difference most likely lies in the selection function and/or sample modelling

# Internal mass calibration with DES

## Comparing mass calibrations

Most Planck clusters are also in the eRASS1 catalogue, with masses derived from the eROSITA cosmological pipeline that also relies on DES shear profiles for mass calibration

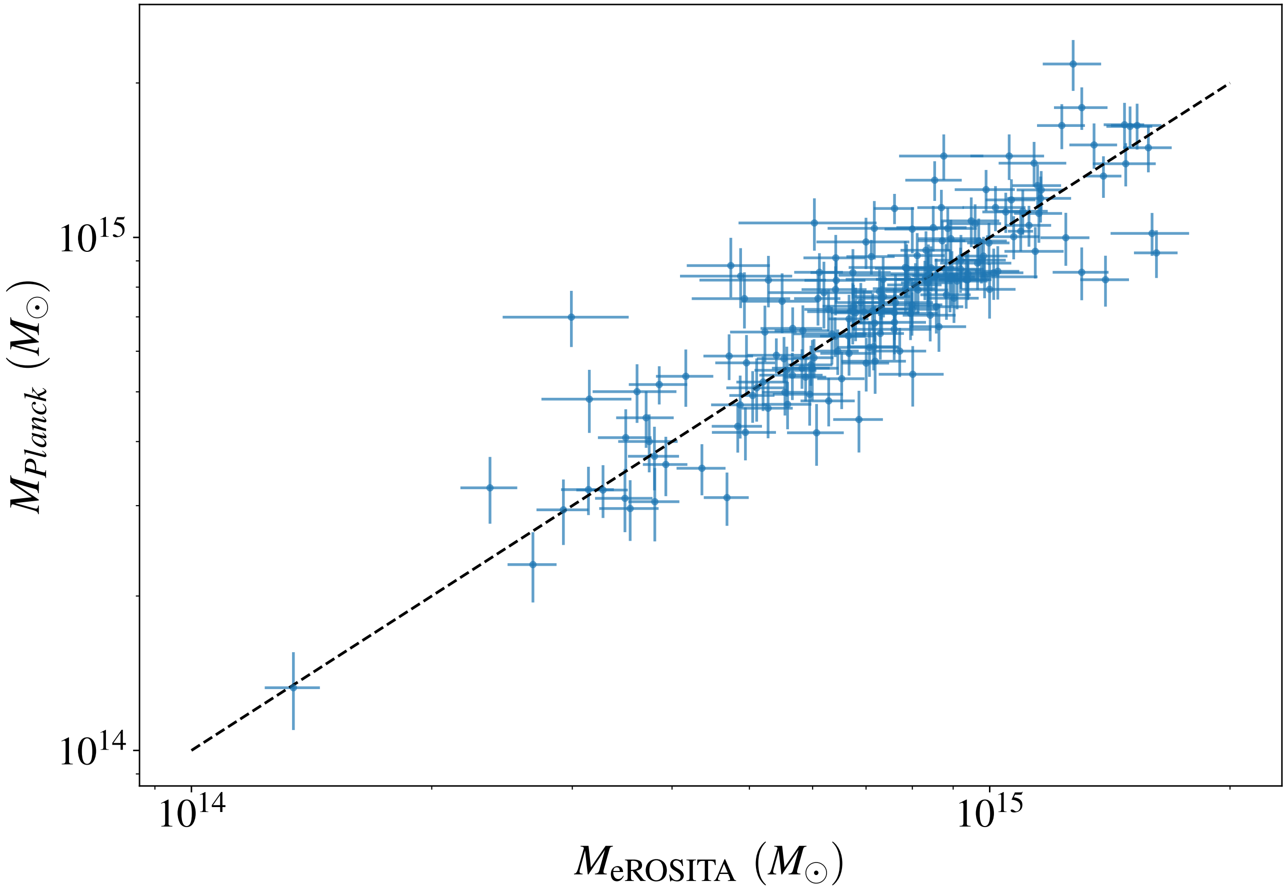


Comparing masses from eROSITA+DES and Planck+DES confirms that the mass calibration is consistent

# Updating the mass calibration of the Planck cluster sample

## Take-home messages

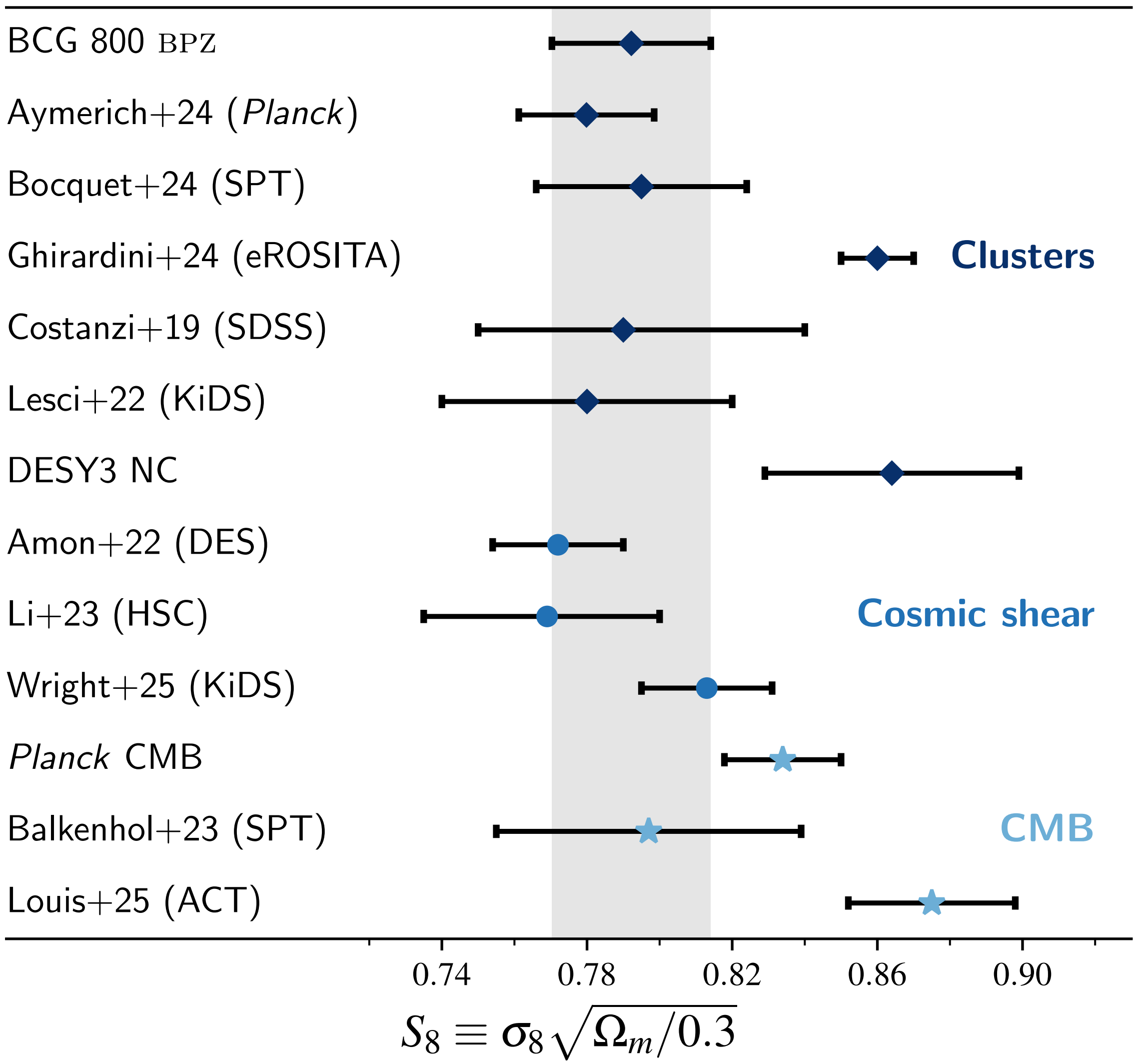


- Constraints derived with **pointed CFHT WL observations and DES shear profiles are coherent**
- Choice of X-ray telescope doesn't change the final results
- **Coherent constraints** with previous Planck and SPT results
- **Coherent mass calibration** with eRASS1
- **Final constraints in tension** with eRASS1 results
- Difference likely coming from the **sample and/or modelling**
- **Hydro bias in the expected range from simulations:** $(1 - b) = 0.84 \ - 0.89$ depending on WL sample



arXiv:2509.02068

# Visualising tensions in terms of number counts

Because the mass calibrations are consistent,
we can predict Planck number counts with the eROSITA and SPT cosmologies

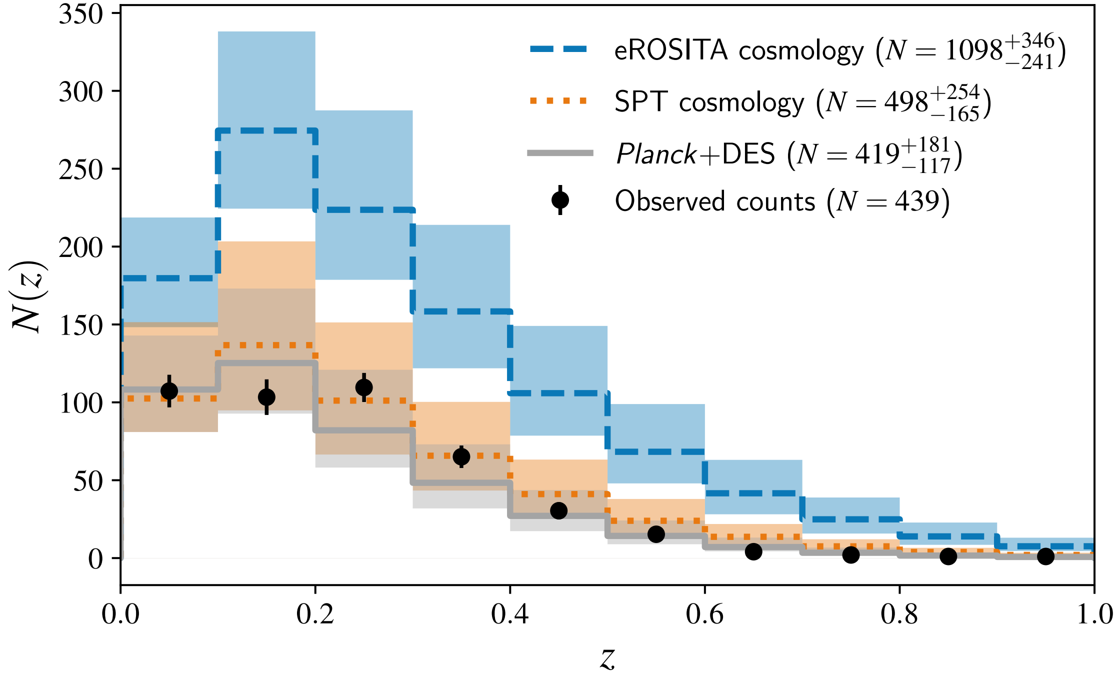


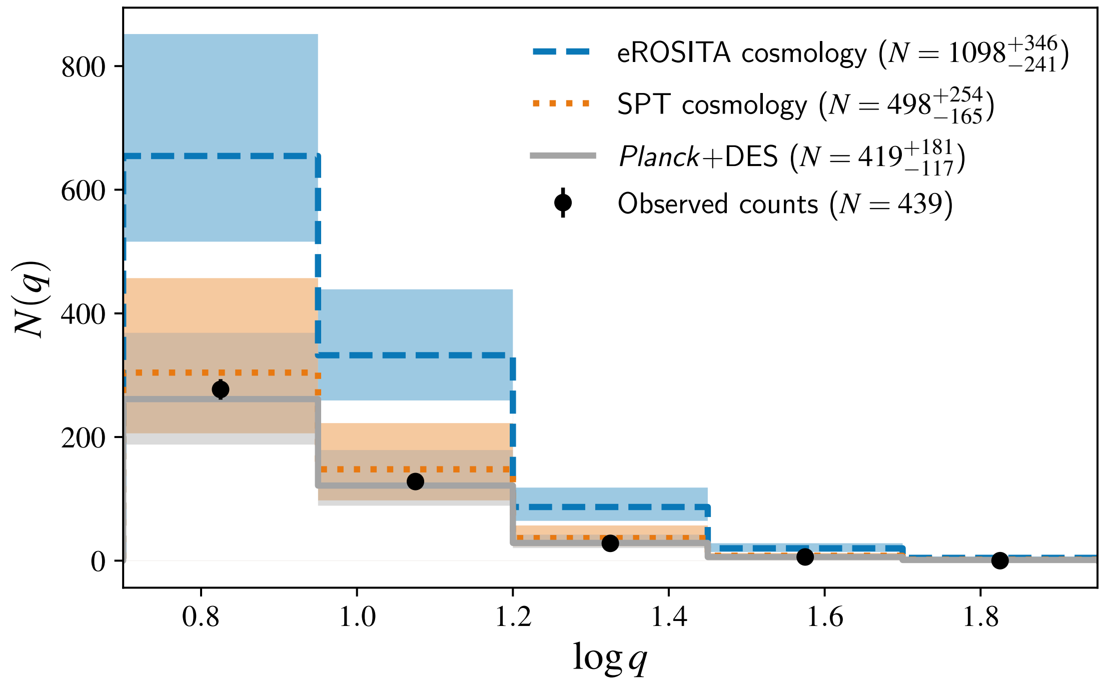


**eROSITA cosmology corresponds to 2.5 times more clusters in the Planck sample**
**SPT is very consistent**

arXiv:2509.08673